

INTERACTION OF LASER RADIATION WITH MATTER. LASER PLASMA

PACS numbers: 42.81.Cn; 72.20.Ht; 72.40.+w
DOI: 10.1070/QE2001v031n03ABEH001924

UV laser-induced current in germanosilicate fibres with built in electrodes

A O Rybaltovskii, V N Bagratashvili, P V Chernov,
P G Kazanskii, V Pruneri, S I Tsypina, Yu S Zavorotnyi

***Abstract*. The nature of photocurrents is studied in germanosilicate single-mode fibres with built in electrodes. It is shown that irradiation by excimer KrF laser pulses at electric field strengths up to 1.6 MV cm^{-1} causes a charge formation and transfer in the core of the fibre and the injection of photoelectrons from metal electrodes to the fibre cladding. Both effects facilitate the flow of electric current through the sample. The dependences of the photocurrent on the electric field strength, the energy density in the laser pulse, the fibre temperature, and the impurity hydrogen in the fibre core are obtained.**

Keywords: *single-mode fibre, electric field, germanium oxygen-deficient centre, laser radiation, photocurrent.*

1. Introduction

The generation and separation of charges in fused silica and fibres under UV laser irradiation are actively studied in view of important applications of these effects in optoelectronics. First of all, these effects are used for the formation of gratings of quadratic nonlinear susceptibility $\chi^{(2)}$ in glass and allow one to improve the SHG efficiency in single-mode germanosilicate glass fibres [1]. In addition, the photoionisation of germanium oxygen-deficient centres (GODCs) in germanosilicate glass (GSG) is one of the dominant mechanisms of its photosensitivity – a phenomenon employed to write the refractive index gratings [2]. Controlling the electron transfer in an external electric field allows the improvement of the photosensitivity of fibres [3, 4]. Finally, the application of these phenomena for the production of fibre electro-optical modulators was considered [5] and a new simple technique was proposed for autocorrelation measurements of the duration of UV femtosecond pulses [6].

Mechanisms of photoinduced generation and separation of charges in pure silica and germanosilicate glasses were studied in Refs [7 – 12]. The main experimental data were obtained in these papers by recording the photoconductivity and luminescence [7 – 9] and also by measuring the absorption and EPR spectra [10] of the centres interacting with UV radiation. In a GSG, such centres are the GODCs whose two-photon ionisation under KrF laser irradiation in an external electric field [9] induces displacement currents. In this case, the photoconductivity of glass may be quite high, comparable with the conductivity of semiconductors. Moreover, as shown in Ref. [9], the main traps for electrons are the ionised GODCs themselves, along with electronegative Ge^{4+} ions. All these investigations were made with volume and film samples and for electric fields below 10 kV cm^{-1}.

In recent years, considerable progress has been made in the production technology of twin-electrode fibres (TEFs) [3, 5, 11]. Such fibres allow one to produce a strong (up to 10 MV cm^{-1}) electric field along an extended optical path. The use of TEFs allows studying photoinduced processes (in particular, the generation and separation of charges) directly in the optical fibres.

Here, we study for the first time the mechanism of photocurrent generation in single-mode germanosilicate TEFs exposed to high-power KrF laser pulses in a strong external electric field (up to 1.6 MV cm^{-1}). The effects of the TEF temperature, UV radiation intensity, and of the presence of molecular hydrogen in the fibre core on the photocurrent processes are considered.

2. Experimental

The radiation of a KrF laser was directed onto the side surface of a single-mode fibre whose polymer cladding was removed (Fig. 1). The length of the segment under irradiation was 0.5 – 3 cm. The fibre with a core made of GSG (the external fibre diameter was 125 μm, the core diameter was 3 μm, the molar content of GeO_2 was 18 %) had two hollow channels 50 μm in diameter. Gold-coated tungsten wire electrodes 25 μm in diameter were loosely fitted into these channels. The minimal distance d between the channel walls was 10 μm. The reflecting fibre cladding was made of 'dry' fused silica containing the OH groups at a level of 50 ppm.

The electrodes were connected to a high-voltage power supply at the opposite ends of the fibre to avoid the air breakdown. The field induced by the TEF electrodes is not uniform over the section of the sample. However, considering the electrode diameter-to-separation ratio, the field in the core of this TEF can be treated as uniform and estimated as $E = U/d$. The peak electric intensity E in the fibre

A O Rybaltovskii, P V Chernov, Yu S Zavorotnyi D V Skobeltsyn Research Institute of Nuclear Physics, M V Lomonosov Moscow State University, Vorob'evy gory, 119899 Moscow, Russia
V N Bagratashvili, S I Tsypina Institute of Laser and Information Technology, Russian Academy of Sciences, Pionerskaya ul. 2, 142190 Troitsk, Moscow oblast, Russia
P G Kazanskii, V Pruneri Optoelectronic Research Centre, University of Southampton, Southampton, S017 1BJ, UK

Received 11 September 2000
Kvantovaya Elektronika **31** (3) 236 – 240 (2001)
Translated by E N Ragozin

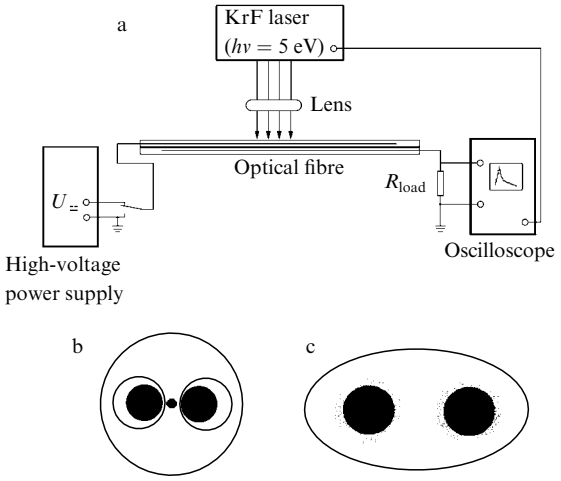

Figure 1. Schematic of the setup for electrical measurements on optical fibres (a) and schematic representations of the cross sections of a germanosilicate single-mode (b) and quartz TEFs (c).

was as high as 1.6 MV cm^{-1} and was limited by electrical breakdown during UV irradiation.

In several experiments, we used fibres with an external diameter of 400 μm synthesised of pure silica. Two electrodes made of nickel wire 100 μm in diameter were alloyed in these fibres at a distance of 120–150 μm from each other (Fig. 1c).

The photocurrent signals induced in the fibre by UV laser pulses were recorded with an S9-8 storage digital oscilloscope. It was simultaneously possible to observe the signal of triplet photoluminescence from GODCs with a maximum at 400 nm [9]. To do this, one of the end faces of the fibre was coupled to an FEU-100 photomultiplier via an appropriate filter.

The sample under study was connected to a dc voltage source via a current-measuring resistor R_{load} (10–100 kΩ) (Fig. 1). During the laser pulse, the oscilloscope loaded with a resistor R_{load} recorded an exponential pulse with the amplitude U and the characteristic duration τ. The magnitude of τ was determined by the response time of the measuring circuits and was much longer than the duration τ_L of the laser pulse (20 ns) and the carrier lifetime in the silica and GSG. The current averaged over a pulse time was calculated from the pulse amplitude U as $I = \tau U/R_{load}\tau_L$.

To analyse processes occurring in the interelectrode space, a sample was irradiated by a series of pulses (N = 10 – 100 pulses) for each field strength E, sample temperature, and UV energy density Φ. Then, the same irradiation was performed for $E = 0$. (The voltage source was replaced with a conductor.) The resultant series will be referred to as $I_{for}^{(N)}$ and $I_{rev}^{(N)}$, respectively. To eliminate the influence of the GODC density variation on the magnitude of the photocurrent signal during laser irradiation, the fibre segment under study was pre-exposed to several tens of laser pulses in the absence of the electric field. During this exposure, the majority of photosensitive GODCs were decayed [9, 13].

The volt–ampere characteristics (VACs) in the form $I_{for}^{(1)}(E)$ and $I_{rev}^{(1)}(E)$ were measured at temperatures of −140, 20, 130, and 300 °C. To measure the VACs at temperatures below room temperature, the sample was placed in a special cell cooled by liquid nitrogen. To heat a TEF to temperatures above room temperature, a convective hot air flow was used.

The effect of the molecular hydrogen introduced into the glass network on the photocurrent generation was studied by using TEFs exposed to the hydrogen atmosphere at a pressure of 60 bar and a temperature of 20°C for two weeks. This provided the concentration of H_2 molecules in the core at a level of 7×10^{19} cm^{-3} [14].

3. Results and discussion

The pulsed UV laser irradiation of single-mode TEFs produces photocurrent pulses in them, whose amplitude depends on the applied voltage U, the energy density Φ in the laser pulse, the sample temperature T, and the number N of laser pulses.

For the energy density in the laser pulse $\Phi = 150$ mJ cm^{-2}, the strength of the external electric field $E = 1.36$ MV cm^{-1}, the load resistance $R_{load} = 100$ kΩ, and the pulse duration $\tau = 17$ μs determined by the parameters of the recording system, the typical charge was ~ 10 pC and the averaged current I was ~ 500 μA. According to our previous investigations [9], the main contribution to the photocurrent signal is made by the electrons produced by the ionisation of GODCs in the fibre core, which move in the external electric field.

3.1. Screening effect and emission current

As the fibre is repetitively exposed to laser pulses, the amplitude of photocurrent pulses decreases for any strength of the applied electric field. This is a consequence of the screening of the external electric field by the induced internal field, which is related to the macroscopic charge separation and their localisation at the core-cladding interface [9]. This current, which is a displacement current, is denoted as A_1 in Fig. 2. Note that this decrease is, for $T = 300$ K, $\Phi = 150$ mJ cm^{-2}, and $E = 616$ kV cm^{-1}, within 50 % of the amplitude of the first pulse $I_{for}^{(1)}$. This implies that the screening is incomplete, unlike the data of Ref. [9] where volume glass samples exhibited a complete screening of the external field. In Fig. 2, the saturation photocurrent of the sequence $I_{for}^{(N)}$ is denoted as B.

We also noticed that $I_{for}^{(1)} - B = I_{rev}^{(1)}$ for virtually all E and Φ. Therefore, the total photocurrent signal $I_{for}^{(N)}(E)$ for

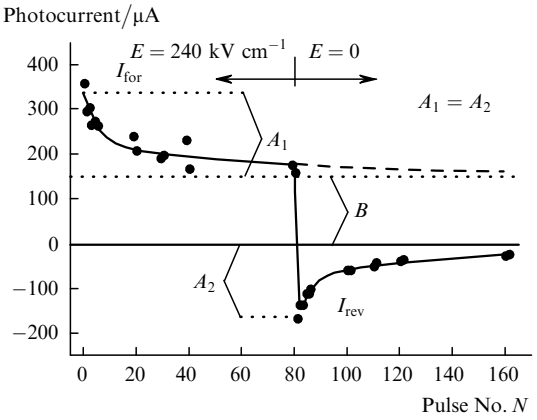

Figure 2. Typical form of the pulsed photocurrent as a function of the laser pulse number.

the fibres under study involves, in addition to the displacement current A_1, a constant component $B(E)$. This component is in essence a 'transit current', i.e., cannot be explained on the basis of displacement currents.

The relative contribution of the transit current, i.e., the quantity $B/(A_1 + B)$, depends strongly on the sample temperature. For instance, for $T = -140\,^{\circ}\mathrm{C}$ and $E = 0.75$ MV cm^{-1}, the photocurrent decays virtually to zero by the twentieth irradiation pulse. At room temperature, the transit photocurrent component, on the contrary, strongly increases. Moreover, the resultant data imply that the relative contribution of the transit current increases with the field intensity E and the energy density Φ of the laser pulses. In our view, the transit current is associated with the photoemission of electrons when the radiation hits the metal electrodes.

The question of the contribution of the emission current to the total photocurrent has already been discussed for planar silica waveguides with a high content of germanium and phosphorous [8]. A crude estimate of the emission charge made by the formula $q = \eta\Phi S/h\nu$ (η is the efficiency of photoelectron emission per one absorbed photon, which is equal for many metals to about 10^{-4} [15] for a photon energy close to the work function $h\nu_0$, $S = 10^{-3}$ cm^2 is the irradiation surface area, and $\Phi = 150$ mJ cm^{-2}) gives a value of 3 nC. This estimate overrates the emission charge because it pertains, first, to the saturation current when all electrons are collected and, second, to the electron emission in vacuum. In our case, the emission occurs from gold electrodes into fused silica.

To elucidate the role of the emission current component, we performed several experiments to measure the dependences $I_{\mathrm{for}}^{(N)}$ in thick fibres and volume glass samples, which allowed us to irradiate glass without hitting the electrodes. As a result, we found that upon such irradiation, the contribution of the transit current substantially decrease whereas the displacement currents A_1 and A_2 remain invariable. This confirms the emission nature of the transit current.

Fig. 3a gives VACs $I_{\mathrm{for}}^{(1)}(E)$ and $I_{\mathrm{rev}}^{(1)}(E)$ for the photocurrent in an TEF. One can see that a portion of the curve $I_{\mathrm{for}}^{(1)}(E)$ exhibits a superlinear dependence on the electric field strength when E is large enough. In accordance with the notions of Ref. [16], the superlinear (quadratic) form of a VAC is realised when charges are injected from electrodes into a dielectric and its electric neutrality is violated in the process. In our case, we can say that the photoemission electrons from gold electrodes are injected into the pure silsca of the TEF cladding under the UV irradiation.

This is qualitatively confirmed by the results of the following experiment. An TEF was excited through the end face and not through the side surface. Both wire electrodes were connected together and were under the same voltage, which ruled out the photocurrent arising from the participation of the charge carriers produced in the TEF core. The second circular electrode of tin was deposited on the outside, at 2 cm from the end face under irradiation. The external tin electrode was screened from the UV radiation with a special stop. Fig. 3b shows the VACs obtained with this experimental setup. One can see that a portion of the curve $I_{\mathrm{for}}^{(1)}(E)$ exhibits a nearly quadratic dependence on the field strength. Therefore, the experimental dc dependences $I_{\mathrm{for}}^{(1)}(E)$ and sequences $I_{\mathrm{for}}^{(N)}$ characterise not only the motion of charge carriers in the TEF core, but the emission currents from the electrodes as well.

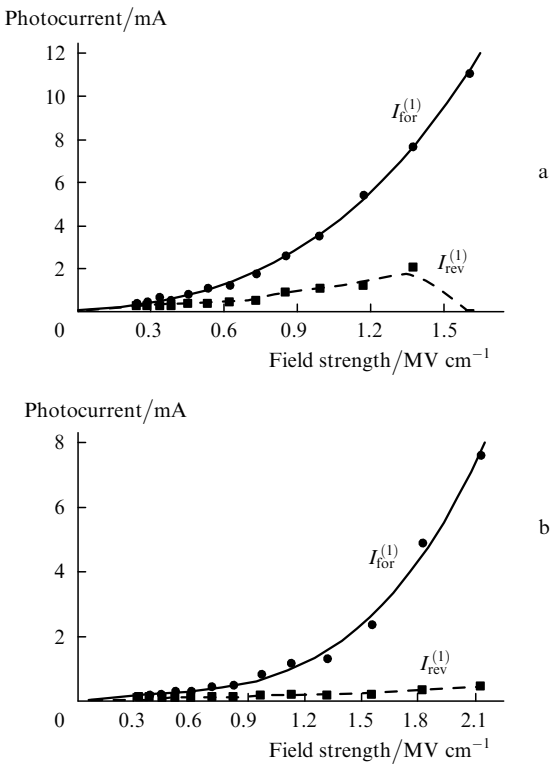

Figure 3. Volt – ampere characteristics of direct and reverse photocurrents when the field is localised in the TEF core (a) and cladding (b).

3.2. Temperature effect

The curves in Fig. 4 show some of the features of production of the charge induced in the TEF core for different temperatures of the sample under irradiation. First of all, this is the existence of a maximum of the displacement current $I_{\mathrm{rev}}^{(1)}$ for $T = 130^{\circ}\mathrm{C}$ (Fig. 4a). In this case, the current $I_{\mathrm{rev}}^{(1)}$ proves to be 1.5 – 2 times higher than it is at room temperature. For $T = 300^{\circ}\mathrm{C}$, the current $I_{\mathrm{rev}}^{(1)}$ (and hence the screening internal field) is significantly lower, which can be attributed primarily to the temperature enhancement of recombination of the charges separated. A several-fold reduction in the total dc photocurrent signal was also observed at this temperature.

Note that in fused silica heated to such temperatures, there occurs, according to Ref. [11], the process of thermopoling – the charge transfer in the electric field. As a result of the thermopoling, the external field in the electrode gap is compensated for, which in turn should lead to a reduction in the photocurrent signal observed in our experiment.

In addition, we directly detected the appearance of a thermally induced field in fibres heated to 300 – 500 °C at the applied field strength of 1.0 – 1.4 MV cm^{-1} and measured its intensity. The recording proceeded as fol-lows: after a thermopoling, the fibre was cooled to room temperature, then the voltage source was replaced with a conductor and a UV laser was employed to induce a sequence $I_{\mathrm{therm}}^{(N)}$ of reverse current pulses, which was only slightly different from the sequence $I_{\mathrm{rev}}^{(N)}$ of photocurrent pulses obtained in the photopoling for the same voltage across the electrodes.

As for low-temperature measurements, a comparison of the curves in Fig. 4b shows that the amplitude of photocurrent pulses due to the induced charge for $T = -140^{\circ}\mathrm{C}$ proves, on the whole, to be lower than in room-temperature

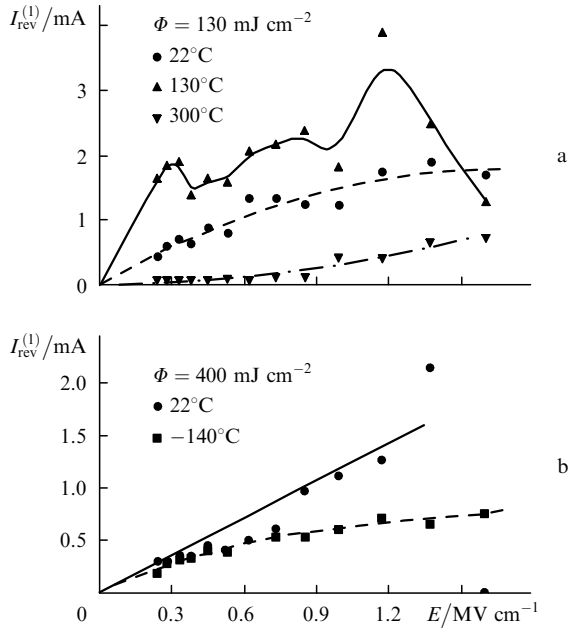

Figure 4. Amplitude of the induced charge as a function of the electric field strength for $\Phi = 130$ (a) and 400 mJ cm^{-2} (b) and different temperatures of the optical fibre under irradiation.

experiments. With decreasing temperature, the probability that electrons are captured by intermediate traps is likely to rise, with the effect that their free path shortens. It is pertinent to note that the photocurrent signal $I_{for}^{(1)}$ from the fibre under irradiation dropped nearly to zero when the temperature of the sample was lowered to the liquid nitrogen temperature, i.e., lowering the temperature supposedly reduced the contribution of the emission current as well.

3.3. Effect of hydrogen

In fibres pre-saturated with molecular hydrogen, the production of induced charge and its relaxation under UV irradiation proceed simultaneously with photochemical reactions involving H_2 molecules in the $SiO_2 : GeO_2$ matrix. It has been known [13, 17] that photoinduced reactions of H_2 molecules with colour centres can strongly alter the defect composition of glass, resulting in the photochemical incorporation of hydrogen atoms in the glass matrix and the appearance of defects of the $\equiv$Si−OH and $\equiv$Ge−OH types. Fig. 5 depicts the dependences $I_{rev}^{(N)}$ in the initial samples and hydrogen-saturated samples. One can see two obvious differences: the hydrogen-bearing samples exhibit, first, a growth of the photocurrent signal $I_{rev}^{(1)}$ and, second, an evident increase in the rate of induced-charge relaxation with a pulsed UV excitation in a zero external field.

These results can be interpreted in the following way. Under UV irradiation, in the germanosilicate glass network there occur photochemical reactions involving H_2 molecules, with the effect that hydrogen 'builds up' the defects, which are potential electron traps. In this case, the free electron path in the glass lengthens, resulting in the increase in the GSG photoconductivity. As a result, the charge transferred in one pulse increases and, accordingly, the induced-charge relaxation speeds up. An increase in the electron free path and their lifetime after the excitation in a silica with an enhanced content of $\equiv$Si−OH hydroxyl

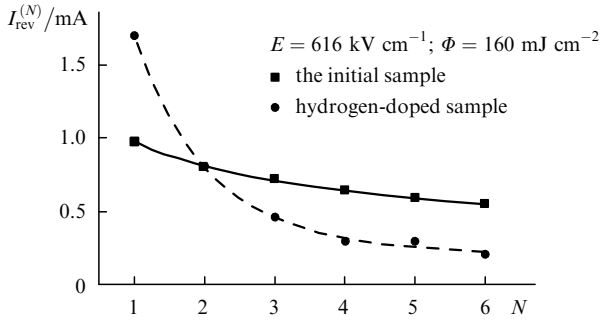

Figure 5. UV laser-stimulated relaxation of the induced charge in the initial sample and in the sample processed in hydrogen; $E = 616$ kV cm^{-1} and $\Phi = 160$ mJ cm^{-2}

groups was noted by the authors of Ref. [18]. These results were treated as a consequence of the reduction of the electron trap density arising from their modification by hydrogen in the SiO_2 matrix.

4. Conclusions

The experimental investigation of UV laser-induced photocurrent production in germanosilicate fibres with built in electrodes in a strong external electric field performed in our work allowed us to establish the following principal features of the process. Under UV irradiation of the TEF, first of all there occurs a production of free electrons in the fibre core due to the GODC ionisation and a macroscopic separation of charges with their possible localisation at the core–cladding interface. This results in the screening of the external electric field by the internal field of the charges separated.

In addition, the photoelectrons from the wire electrodes are injected into the pure silica of the fibre cladding. The contribution of the emission components to the total photocurrent signal increases with electric field strength and energy density in the laser pulse.

Electron traps play a significant part in the separation of charge carriers. The efficiency of capture of UV-induced electrons by the traps depends on the temperature of the TEF under irradiation and also on the chemical composition of its core glass. The modification of the electron traps caused by the incorporation of hydrogen molecules is responsible for the growth of a photocurrent signal and the acceleration of the relaxation of a UV laser-induced charge in the internal field. Lowering the sample temperature below room temperature favours a fast electron capture even by a small trap and, as a consequence, a reduction of its free path and the photocurrent pulse height.

Acknowledgements. The authors thank V A Bogatyrev of the Fibre Optics Research Centre at the General Physics Institute, Russian Academy of Sciences, for helpful discussions and for providing fibre samples with built in nickel wire electrodes. This work was supported by the Russian Foundation for Basic Research (Grant Nos 98-02-16728 and 97-02-17244) and the Program for the Support of Leading Scientific Schools of the Russian Federation (Grant No. 00-15-96596).

References

1. Bergot M-V, Farries M C, Fermann M Z, Li L, Pointz-Wright L Y, Russel P St J, Smithson A *Opt. Lett.* **13** 592 (1988)
2. Hand D P, Russel P St J *Opt. Lett.* **15** 102 (1990)
3. Guiquempas Y, Martinelli G, Niay P, Bernage P, Douay M, Bayen J F, Poignant H *Opt. Lett.* **24** 139 (1999)
4. Rybaltovskii A O, Zavorotnyi Yu S, Chernov P V, Bagratashvili V N, Tsypina S I, Kazanskii P G *Appl. Phys. Lett.* **77** 1578 (2000)
5. Fujiwara T, Wong D, Zhao Y, Fleming S, Poole S, Sceats M *Electron. Lett.* **31** 573 (1995)
6. Streltsov A M, Ranka J K, Gaeta A L *Opt. Lett.* **23** 798 (1998)
7. Dianov E M, Kazansky P G, Starodubov D S, Stepanov D Yu *Sov. Lightwave Commun.* **2** 269 (1992)
8. Kashyap R, Maxwell G D, Williams D I *Appl. Phys. Lett.* **62** 214 (1993)
9. Bagratashvili V N, Tsypina S I, Chernov P V, Rybaltovskii A O, Zavorotnyi Yu S, Alimpiev S S, Simanovskii Ya O, Dong L, Russel P St J *Appl. Phys. Lett.* **68** 1616 (1996)
10. Takanashi M, Fujiwara T, Kawachia T, Ikashima A J *Appl. Phys. Lett.* **71** 993 (1997)
11. Kazansky P G, Russel P St J, Takabe H *J. Lightwave Technol.* **15** 1 (1997)
12. Hughes R G *Radiat. Eff.* **26** 225 (1975)
13. Zavorotnyi Yu S, Rybaltovskii A O, Chernov P V, Bagratashvili V N, Popov V K, Tsypina S I, Dong L *Fiz. Khim. Stekla* **23** 629 (1997)
14. Bagratashvili V N, Tsypina S I, Chernov P V, Rybaltovskii A O *J. Phys. Chem.* **99** 6640 (1995)
15. Sommer A H *Photoemissive Materials: Preparation, Properties, and Uses* (New York: Wiley, 1968)
16. Lampert M A, Mark P *Current Injection in Solids* (New York: Academic Press, 1970)
17. Dianov E M, Starodubov D S, Frolov A A, Rybaltovskii A O *Kvantovaya Elektron.* **23** 565 (1996) [*Quantum Electron.* **26** (6) 550 (1996)]
18. Silin' A P, Trukhin A N *Tochechnye Defekty v Kristallicheskom i Stekloobraznom SiO_2* (Point Defects in Crystalline and Vitreous SiO_2) (Riga: Zinatne, 1985)